Real-time analysis of endogenous protoporphyrin IX fluorescence from δ-aminolevulinic acid and its derivatives reveals distinct time- and dose-dependent characteristics *in vitro*

Tobias Kiesslich
Linda Helander
Romana Illig
Christian Oberdanner
Andrej Wagner
Herbert Lettner
Martin Jakab
Kristjan Plaetzer

Real-time analysis of endogenous protoporphyrin IX fluorescence from δ-aminolevulinic acid and its derivatives reveals distinct time- and dose-dependent characteristics *in vitro*

Tobias Kiesslich,[a,b] Linda Helander,[c] Romana Illig,[d] Christian Oberdanner,[e] Andrej Wagner,[b] Herbert Lettner,[f] Martin Jakab,[a] and Kristjan Plaetzer[g,*]

[a]Paracelsus Medical University, Institute of Physiology and Pathophysiology, Strubergasse 21, Salzburg A-5020, Austria
[b]Paracelsus Medical University/Salzburger Landeskliniken, Department of Internal Medicine I, Muellner Hauptstrasse 48, Salzburg A-5020, Austria
[c]Norwegian University of Science and Technology, Department of Cancer Research and Molecular Medicine, Erling Skjalgssons gate 1, N-7491 Trondheim, Norway
[d]Paracelsus Medical University/Salzburger Landeskliniken, Institute of Pathology, Muellner Hauptstrasse 48, Salzburg A-5020, Austria
[e]Tecan Austria, Untersbergstrasse 1, Grödig A-5082, Austria
[f]University of Salzburg, Department of Materials Science and Physics, Division of Physics and Biophysics, Hellbrunnerstraße 34, Salzburg A-5020, Austria
[g]University of Salzburg, Department of Materials Science and Physics, Laboratory of Photodynamic Inactivation of Microorganisms, Hellbrunnerstraße 34, Salzburg A-5020, Austria

Abstract. Photodynamic therapy (PDT) and photodiagnosis based on the intracellular production of the photosensitizer protoporphyrin IX (PPIX) by administration of its metabolic precursor δ-aminolevulinic acid (ALA) achieved their breakthrough upon the clinical approval of MAL (ALA methyl ester) and HAL (ALA hexyl ester). For newly developed ALA derivatives or application in new tumor types, *in vitro* determination of PPIX formation involves multiparametric experiments covering variable pro-drug concentrations, medium composition, time points of analysis, and cell type(s). This study uses a fluorescence microplate reader with a built-in temperature and atmosphere control to investigate the high-resolution long-term kinetics (72 h) of cellular PPIX fueled by administration of either ALA, MAL, or HAL for each 10 different concentrations. For simultaneous proliferation correction, A431 cells were stably transfected with green fluorescent protein. The results indicate that the peak PPIX level is a function of both, incubation concentration and period: maximal PPIX is generated with 1 to 2-mM ALA/MAL or 0.125-mM HAL; also, the PPIX peak shifts to longer incubation periods with increasing pro-drug concentrations. The results underline the need for detailed temporal analysis of PPIX formation to optimize ALA (derivative)-based PDT or photodiagnosis and highlight the value of environment-controlled microplate readers for automated *in vitro* analysis. © *2014 Society of Photo-Optical Instrumentation Engineers (SPIE)* [DOI: 10.1117/1.JBO.19.8.085007]

Keywords: photodynamic therapy; photodiagnosis; protoporphyrin IX; δ-aminolevulinic acid; formation kinetics; automated analysis.

Paper 140262R received Apr. 25, 2014; revised manuscript received Jun. 17, 2014; accepted for publication Jul. 14, 2014; published online Aug. 12, 2014.

1 Introduction

Photodynamic therapy (PDT) based on the δ-aminolevulinic acid (ALA) is considered as one of the most selective treatments for dermatological precancers or early stage malignancies.[1,2] This pro-drug concept represents an alternative approach to the direct (systemic) administration of a photosensitizing agent: the presence of exogenous ALA bypasses the negative feedback in heme biosynthesis and results in accumulation of the endogenous photosensitizer (PS) protoporphyrin IX (PPIX)—preferentially in neoplastic cells. PDT using ALA-induced PPIX offers advantages over other PS including low overall photosensitization, very good cosmetic results, and little risk of overtreatment due to increased photobleaching of PPIX during prolonged illumination.[3] In 1999, ALA-PDT gained FDA approval for treatment of actinic keratoses. In addition to direct tumor treatment by photochemical reactions, the emission of secondary photons of ALA-induced PPIX is also successfully employed in photodiagnosis,[4–6] i.e., the identification of malignant tissue by its red fluorescence including the option of its removal via fluorescence-guided resection. However, despite of promising preclinical data, photodynamic procedures based on the ALA failed to achieve further approvals. Among other reasons, the zwitterionic character of ALA under physiological conditions—negative charge at the carboxylic terminus and positively charged at the amino end—and the related limited capacity to diffuse through lipophilic biological membranes has been identified as a major drawback of ALA. This aspect may explain low tissue penetration depth, nonhomogenous distribution of PPIX following topical application as well as the limited response of noduloulcerative basal cell carcinoma to ALA-PDT.[2,7]

Newly introduced lipophilic ALA derivatives have overcome these limitations. Along with much better tissue penetration, lipophilic derivatives instead of the original ALA yield higher

*Address all correspondence to: Kristjan Plaetzer, E-mail: kristjan.plaetzer@sbg.ac.at

amounts of intracellular PPIX, which, in turn allows for shorter incubation periods and/or lower concentrations of the pro-drug.[8–12] Furthermore, unwanted side effects of ALA-PDT such as pain sensation during illumination could be reduced when using ALA derivatives.[13,14] Given the molecular properties of ALA, a number of ALA derivatives with different physico-chemical and pharmacokinetic properties may be suggested (for an excellent overview see Ref. 15). A majority of the *in vitro* and clinical data is available for two ALA esters, ALA methyl ester (MAL) and ALA hexyl ester (HAL). Both substances received approvals by health authorities: MAL (Metvix®) for treatment of actinic keratoses and basal cell carcinoma (EU, Norway, and Australia), for treatment of actinic keratoses in the US (under the trademark Metvixia®) and HAL in the US (Cysview®) and the EU (plus Norway and Iceland; Hexvix®) for photodiagnosis of bladder cancer.[15]

Various studies investigated the *in vitro* formation kinetics of PPIX from either ALA, MAL, or HAL in (tumor) cells. It is well established that the ALA and most likely MAL are transferred into the cytoplasm by dipeptide and tripeptide transporters.[16–21] In contrast, uptake of the more lipophilic HAL is considered to take place mainly by diffusion and endocytosis.[16] Therefore, PPIX formation kinetics and PPIX accumulation levels depend on several parameters including cell type, pro-drug concentration, and time point postadministration. As a consequence, the *in vitro* analysis of (new) ALA derivatives as the first step becomes multiparametric; for example, the incubation concentration and period, the medium (pH value, serum content), and the cell line(s) (tumor type and corresponding nonmalignant model system) may raise the number of samples required for a detailed analysis beyond a level of manageability. In order to reduce complexity, most studies on PPIX formation either treat some parameters, such as the incubation period as constant or examine a limited set of data points only (e.g., PPIX content at a limited number of time points postincubation[22,23]).

To overcome some of the limitations, this study describes an approach of automated long-term analysis of intracellular PPIX formation with a very high temporal resolution. By using a multimode microplate reader equipped with temperature controls and a gas control module, which allows for precise adjustment of the CO_2 partial pressure (to avoid pH shifts of the incubation medium), we recorded the PPIX formation kinetics during 72 h induced by up to 10 different concentrations of ALA, MAL, and HAL in A431 human epidermoid carcinoma cells stably transfected with green fluorescent protein (GFP) for correction of cellular proliferation. With this tool, the PPIX fluorescence of cells treated with more than 40 different conditions (duplicate wells) can be automatically recorded for more than 3 days without any need to interfere with the measurement.

2 Materials and Methods

2.1 Cell Culture and Substances

A431 human epidermoid carcinoma cells (ATCC-No. CRL-1555) were cultured in Dulbecco's modified Eagle's medium (DMEM) with 5% (v/v) fetal bovine serum (FBS) and supplements as previously described[24] in a humidified atmosphere at 37°C and 7.5% CO_2 using cells within 10 passages. To generate an endogenous fluorescing marker for simultaneous determination of the overall cell mass, A431 cells were stably transfected with an expression vector (pEGFP-N1; Takara Bio Europe/Clontech, Saint-Germain-en-Laye, France) encoding for cytoplasmatic GFP using Lipofectin reagent (Invitrogen/Life Technologies, Vienna, Austria) and Geneticin for selection and expansion of stably expressing cell clones according to the manufacturer's instructions. Cells were regularly checked by fluorescence microscopy (IX70 inverted fluorescence microscope; Olympus, Vienna, Austria) for homogeneous and continuous cytoplasmatic expression of GFP. Delta-aminolevulinic acid and ALA methyl ester were purchased from Sigma Aldrich (Vienna, Austria; ALA stock solution 300 mM in Dulbecco's phosphate-buffered saline (DPBS) pH 6.5, MAL stock solution 275.3 mM in DPBS pH 6.5, both stored at −20°C until use). ALA hexyl ester was kindly provided by Photocure (Photocure ASA, Oslo, Norway; stock solution 300 mM in DPBS pH 6.5, −20°C).

2.2 Real-Time Analysis of ALA-Driven PPIX Fluorescence

To ensure minimum evaporation during long-term analysis, cells were cultured in transparent 96 well plates designed with moats at the perimeter of the plate (Edge 96 well plate; Thermo Scientific Nunc, Rochester, New York). These moats were filled with 3 ml of 0.1% w/v agarose (in H_2O) and additional 100-μl H_2O between the wells (Fig. 1). For each experiment, 12,500 A431-GFP cells were seeded in 100-μl 5% FBS DMEM. "Blank values" represent wells with medium but without cells or ALA precursors. From this point on, all washing and incubation steps were performed using phenol red-free DMEM without FBS. Twenty-four hour after seeding, cells were washed with 100-μl DMEM and incubated with varying concentrations of ALA (0.008 to 4.000 mM), HAL (0.001 to 0.500 mM), or MAL (0.008 to 4.000 mM) using a total volume of 250 μl per well in duplicates per plate. Afterward, the microplate was sealed on three sides using Parafilm and the fluorescence measurements were started using an Infinite M200 PRO multimode microplate reader equipped with gas control module (Tecan, Groedig, Austria) and the instrumental settings listed in Table 1 (see also Fig. 1).

2.3 Viability Control Measurements

Following the 72-h measurements, the overall cell viability was assessed using the resazurin assay as previously described.[25,26] This test relies on the reduction of the blue, weakly fluorescent resazurin to the pink, strongly fluorescing resorufin catalyzed by cytochromes and dehydrogenases and is used to indicate overall cellular viability.[27]

2.4 Data Analysis and Presentation

For each experiment, the raw data obtained for the GFP and PPIX fluorescence signal was corrected by subtraction of blank values (250-μl phenol red-free DMEM without FBS, without cells). The PPIX signal was then corrected for the overall cell mass by division by the corresponding GFP value for each well and time point. Mean values from the two replicates per plate were calculated and means $\pm$ SEM from five independent experiments were plotted or used for further calculation. Diagrams and calculations (first deviation) were generated using Microcal OriginPro 9.0 using the Savitzky-Golay filter for smoothing of the derivation curve (OriginLab Corporation, Northampton, Massachusetts).
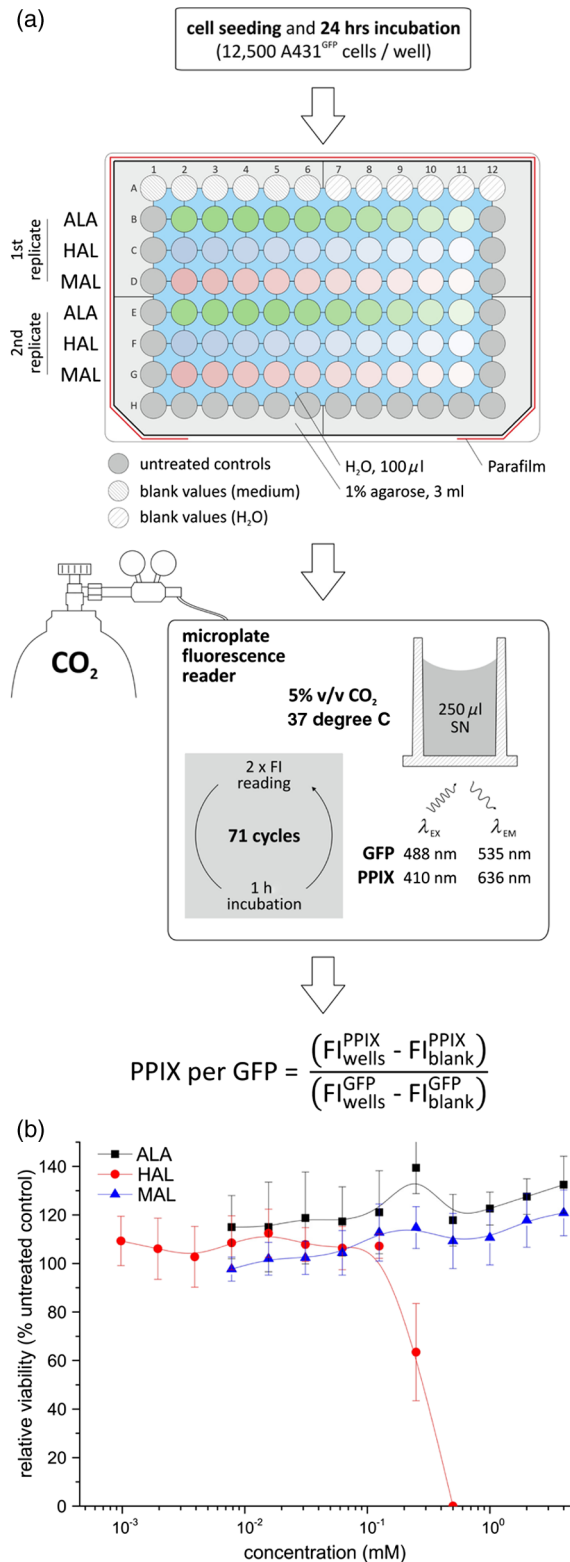
(a)

$$\text{PPIX per GFP} = \frac{\left(FI_{wells}^{PPIX} - FI_{blank}^{PPIX}\right)}{\left(FI_{wells}^{GFP} - FI_{blank}^{GFP}\right)}$$

(b)

Fig. 1 (a) Experimental setup including the plate layout, the measurement conditions, and the data evaluation for long-term monitoring of ALA-induced PPIX formation in A431-GFP cells. Abbreviations: ALA, δ-aminolevulinic acid; FI, fluorescence intensity; GFP, green fluorescent protein; HAL, ALA hexyl ester; MAL, ALA methyl ester; PPIX, protoporphyrin IX; SN, supernatant. (b) Overall viability of A431-GFP cells post 72-h measurement: the viability of A431-GFP cells was analyzed by the resazurin assay immediately after PPIX long-term measurements. Data points represent means related to untreated controls $\pm$ SEM.

3 Results

3.1 Continuous Long-Time Fluorescence Measurements

To investigate the kinetics of PPIX formation, each 10 different concentrations of ALA, MAL, and HAL (in 250-μl phenol red-free DMEM without FBS) were added in duplicates to microplate wells containing A431 cells stably expressing GFP at 24-h postseeding. Afterward, the fluorescence of endogenously formed PPIX and GFP was measured each hour for a total incubation period of 72 h in a microplate reader equipped with a temperature control (set at 37°C) and atmosphere regulation unit providing 5% v/v CO_2. To prevent volume loss of the medium supernatant due to evaporation, humidity was passively maintained by addition of agarose (0.5%, 3 ml) or water (100 μl) in the outer compartments or between the wells of the microplate, respectively. See Fig. 1(a) for an overview of the experimental setup. Control experiments (data not shown) confirmed that in the inner wells of the microplate (B2-G11) the well supernatant volume did not fall below 90% to 95% of the initial value after the 72-h incubation period. Furthermore, the cell viability was checked after the experiment using the resazurin test indicating no loss of viability except for the wells incubated with the two highest concentrations of HAL (1.0 and 2.0 mM) which show considerable dark toxicity [Fig. 1(b)] and were therefore not included in the subsequent analysis.

3.2 Kinetics of ALA-Based Formation of PPIX

Figure 2 shows the formation kinetics of PPIX corrected by the cell's GFP signal correspondingly for each well and time point. For higher concentrations of ALA, MAL, or HAL, the PPIX/GFP signal shows a steady, nearly linear increase during the first 5-h postincubation. For ALA and MAL at concentrations between 0.25 and 2.0 mM [Figs. 2(a) and 2(b)], the slope of the curve decreases after 20 h and reaches a peak at about 30-h post-incubation. For the highest concentration used with these two pro-drugs (4 mM), the kinetics is similar but peaks at earlier time points in the range between 15 and 20 h. Notably, the overall fluorescence signal at 4-mM ALA or MAL is considerably lower than in wells with lower concentrations (i.e., 0.5, 1.0, and 2.0-mM ALA and 1.0 and 2.0-mM MAL). Cells incubated with concentrations below 0.063-mM ALA or 0.125-mM MAL do not show significant PPIX fluorescence signals [Figs. 2(a) and 2(b)]. After reaching the peak signal, the PPIX fluorescence starts to decrease, resulting in values of about 80% of the peak signal between 0.5 and 2.0 mM at 72-h postincubation. This decrease is more pronounced for both the highest concentration (4 mM) and lower concentrations (<0.125 mM). These curves almost reach the baseline fluorescence after 72-h incubation.

In contrast to ALA and MAL, the kinetics of HAL-induced PPIX [Fig. 2(c)] follows a clear dose-dependent characteristic in terms of PPIX fluorescence levels reached during the experiment, otherwise the kinetics show a comparable overall shape. Between 0.004 and 0.016 mM, the fluorescence peak maxima show an approximate doubling with each increase in HAL concentration. At higher concentrations between 0.031 and 0.125 mM, a trend toward saturation is observed, similar to the results with ALA or MAL. Accordant to the two other pro-drugs, the PPIX/GFP signal decreases after the peak value, reaching for some (lower) concentrations baseline levels at 35, 45, and 65-h postincubation for 0.004, 0.008, 0.016-mM HAL, respectively.

Table 1 Instrumental settings of the Tecan Infinite M200 PRO multimode microplate reader employed for measurement of green fluorescent protein (GFP, measure for cell number) and the content of protoporphyrin IX (PPIX).

Parameter	Read mode	λ_{Ex} (nm)	λ_{Em} (nm)	Number of flashes	Integration time (μs)
GFP	Fluorescence bottom	488 ± 9	535 ± 20	25	20
PPIX	Fluorescence bottom	410 ± 9	636 ± 20	25	20

Additionally, the temporal manifestation of the maximum peak signal seems to be dose-dependent with a trend to later time points (about 30 h) for higher concentrations [Fig. 2(c)].

3.3 Curve Analysis of PPIX Formation Kinetics

Figures 3(a)–3(c) show the first derivation of the PPIX fluorescence curves (calculated from values plotted in Figs. 2(a)–2(c). For ALA and MAL, Figs. 3(a) and 3(b) point out that the highest concentration (4 mM) results in a comparably fast kinetics of PPIX formation and breakdown characterized by the steepest decrease in the slope of the PPIX curve. The slopes of the PPIX curves at intermediate concentrations between 2 and 0.125 show a similar zero-crossing point at about 30 h indicating the temporal peak of PPIX formation. The derivative curves of HAL [Fig. 3(c)] strengthen the notion of a clear dose-dependency of the temporal peaks as their zero-crossing points decrease

continuously with decreasing concentration from 30 to 10-h postincubation for 0.125 to 0.004 mM. Similar to the raw data of the PPIX kinetics in Figs. 2(a)–2(c), the maximum PPIX/GFP values shown in Fig. 3(d) confirm the initial observation that the highest concentrations of ALA and MAL show smaller amounts of PPIX formation compared with the lower concentrations of these pro-drugs.

Although ALA and MAL show a distinct peak of maximal PPIX fluorescence at about 1 mM, the evaluable concentrations of HAL (0.125, 0.063, etc.) follow a clear dose-dependency with a direct relationship between pro-drug concentration and amount of PPIX produced by the cells.

3.4 Temporal Maxima of PPIX Formation

As the success of ALA-based PDT and photodiagnosis is dependent on the optimal, i.e., highest ratio of PPIX produced in the
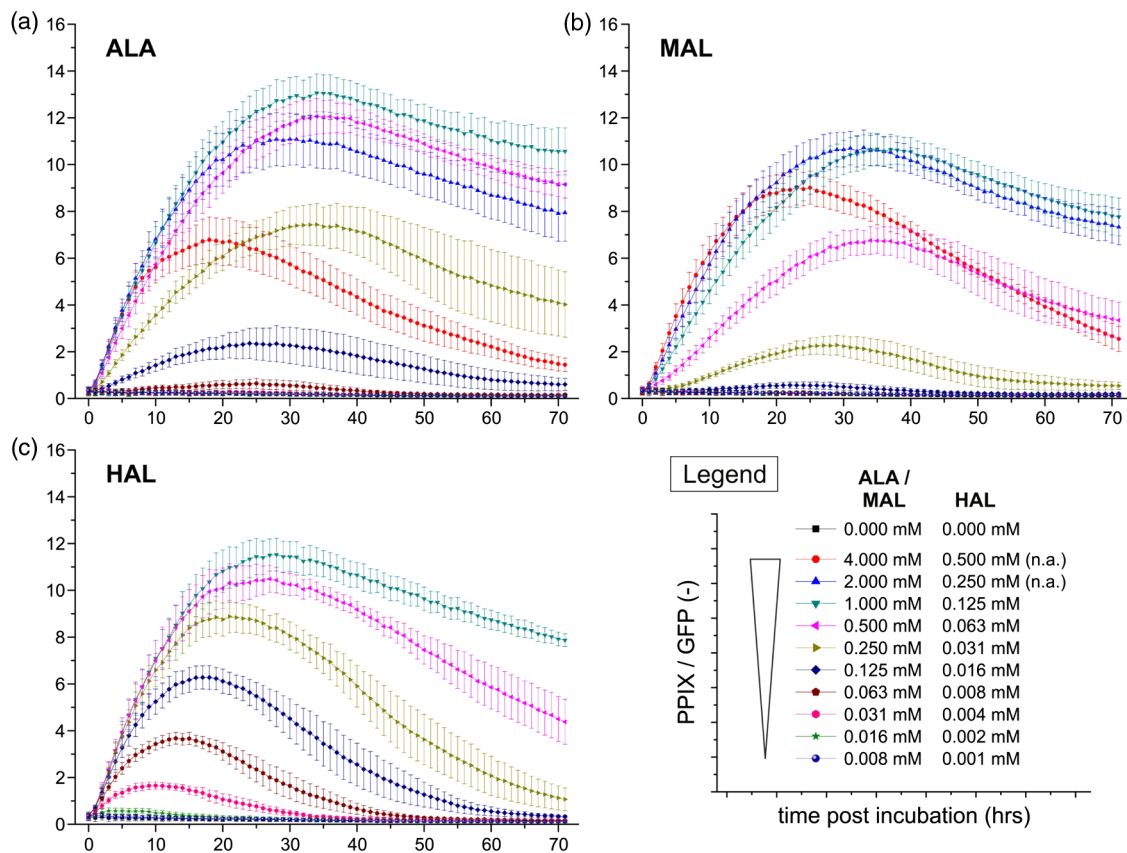

Fig. 2 Time course of protoporphyrin IX fluorescence: A431-GFP cells were incubated with varying concentrations of δ-aminolevulinic acid [ALA; (a) 0.008 to 4.000 mM], ALA methyl ester [MAL; (b) 0.008 to 4.000 mM] or ALA hexyl ester [HAL; (c) 0.001 to 0.125 mM; n.a. = not available] and analyzed for GFP and protoporphyrin IX fluorescence hourly for up to 72-h postincubation. Data points represent the PPIX fluorescence signal related to the corresponding GFP signal as a function of post incubation time. Each data point represents the mean value of five independent experiments $\pm$ SEM.
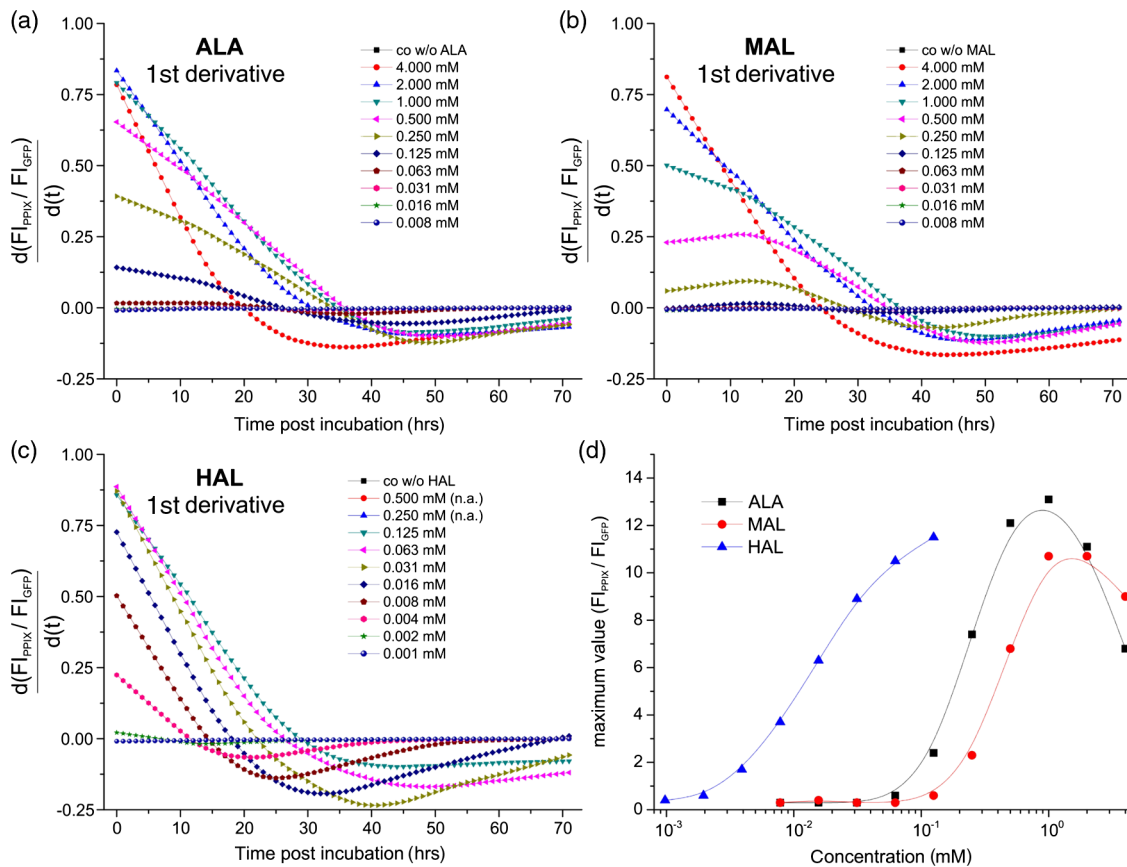
Fig. 3 First derivative and maximal PPIX amount versus ALA concentration: Based on the data of Fig. 2, the first derivative indicating the slope of the original curves is shown in (a–c). Plot (d) depicts the maximum PPIX/GFP value from each kinetics plotted against the concentration of δ-aminolevulinic acid (ALA), ALA methyl ester (MAL), or ALA hexyl ester (HAL).

target (tumor) cells versus healthy tissue, knowledge about pro-drug time and dose-dependency is important for clinical protocol design. To visualize these two parameters determining the conditions of maximal PPIX accumulation, the peak PPIX signal was plotted against the pro-drug concentration and the time point of analysis (Fig. 4, three-dimensional trajectories). This data presentation diagram indicates that the highest PPIX concentration can be induced with 1 to 2-mM ALA or MAL at about 30-h postincubation. As mentioned above, both lower and higher concentrations of these two drugs result in lower PPIX peaks at earlier time points. For the evaluable concentrations of HAL, the peak of PPIX fluorescence occurs at a similar time point, i.e., 25 to 30-h postincubation, yet, requiring a pro-drug concentration one order of magnitude lower (0.125 mM) than those of ALA or MAL.

4 Discussion

The pro-drug concept pursued in ALA-PDT offers a number of benefits for diagnosis and/or treatment of precancers and early stage tumors. It is based on the tumor cell's ability to generate high intracellular amounts of the PS PPIX upon addition of exogenous ALA. Several mechanisms have been suggested as basis for the high tumor selectivity of ALA-PDT observed during clinical application, among which increased transport in proliferating cells and the altered heme metabolism of cancer cells are reported as explanations.[28–31]

Derivatives of ALA with improved lipophilicity potentially increase the passive uptake of the PS pro-drug by diffusion and therefore render cellular incorporation independent of (energy-requiring) transporters such as the PEPT1/2 or GABA transporters, which have been suggested as a shuttle for the zwitterionic ALA.[16–21] As the uptake process is generally considered as the rate-limiting step in PPIX generation from exogenous ALA (and derivatives), higher levels of the PS and, additionally, increased tissue penetration may be achieved if lipophilic ALA derivatives are applied instead of the original substance. Among the possible chemical modifications, formation of ALA esters by reactions of ALA and the corresponding alcohol in the presence of e.g., hydrochloric acid represents a very convenient and simple approach to provide increased lipophilicity of the organic acid. The octanol-water partition coefficients $\left[\log P_{(o/w)}\right]$ of the two most important ALA esters, MAL, and HAL have been measured to be -0.94 for the methyl-ester and 1.84 for the hexyl-ester (ALA: -1.52), indicative of HAL being significantly more lipophilic than MAL.[12]

Our method for recording the PPIX formation kinetics in A431-GFP cells after external application of ALA, MAL, or HAL using a microplate reader equipped with CO_2 regulation presented in this study allows for automated, long-term, and multiparametric analysis of the endogenous PPIX. Our data indicate that using this tool, the PPIX synthesis of cells within each well of a cell culture microplate can be followed for at least 3 days without any need for external manipulation while ensuring environmental conditions almost identical to routine cell culture incubators.
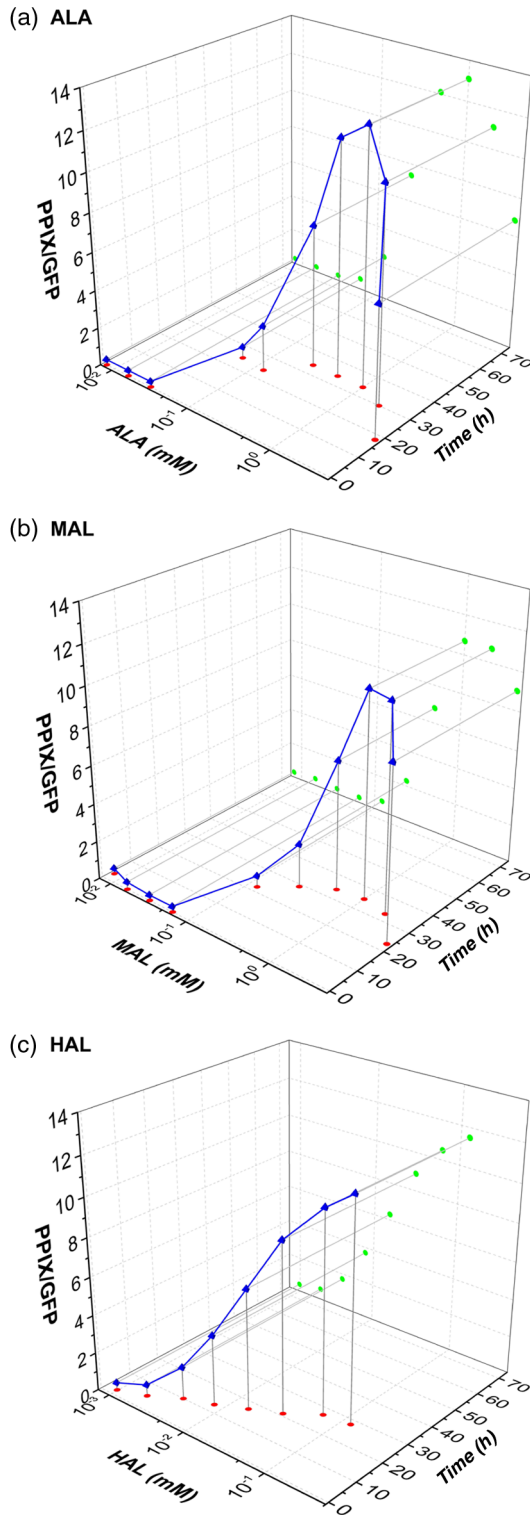
(a) **ALA**

(b) **MAL**

(c) **HAL**

Fig. 4 Maximal PPIX production versus ALA/MAL/HAL concentration and time point: From the data of Fig. 2, three-dimensional trajectory diagrams indicate the maximum of PPIX production for each concentration of δ-aminolevulinic acid [ALA; (a)], ALA methyl ester [MAL; (b)] or ALA hexyl ester [HAL; (c)], and the corresponding time point when the respective maximum value was observed.

Interestingly, the fluorescence of PPIX follows a similar kinetics independent of the pro-drug and its respective concentration (Fig. 2): in a first phase, a very pronounced synthesis of the PS can be observed. For ALA ≥ 0.5 mM, MAL > 1 mM,

and HAL ≥ 31 μM, the amount of PPIX is independent of the pro-drug concentration within the first 10 h, indicating saturation of the enzymatic conversions. The second phase features a peak of intracellular PS: notably, not only the maximal fluorescence depends on the concentration of the ALA (derivative) but also the time point postincubation, at which this peak occurs increased with increasing amount of the pro-drug. This also supports the hypothesis of enzymatic saturation to be relevant for the overall amount of PPIX. In the third phase, a pronounced drop of intracellular PS levels was recorded. This drop is most likely caused by heme formation and other PPIX degradation processes due to a lower PPIX replenishment from upstream conversion and may cause a reduction of the PS to control levels (for example for 8-μM HAL at >50-h postincubation). A comparable kinetics for the first 24 h of incubation was found by Uehlinger et al.[12] using HAL and A549 cells. However, the authors observed a stable plateau phase and no evidence for decreasing PPIX fluorescence after the maximum PPIX value. Furthermore, the cells in that study tolerated much higher concentrations of HAL (up to 2 mM) and the differing results may be caused by the fact that no correction for cell proliferation and that a shorter period of investigation was chosen.

This specific behavior has two main consequences for the (clinical) application: (i) increasing pro-drug concentration does not only increase the amount of PPIX available for treatment or diagnosis but also shifts the temporal maximum to longer incubation periods and (ii) in both, cell culture experiments and clinical application, intracellular PPIX levels drop due to various processes—in other words: our results do not confirm the existence of an extensive (temporal) plateau phase of PPIX as suggested earlier.[32] Both effects are important for the optimization or adaptation of the clinical protocol and have to be considered if different concentrations of ALA (derivatives) are compared at one (or a few) point in time post incubation.

The current data clearly characterize two groups of PPIX precursors in terms of the intracellular PPIX levels and the concentrations of the respective ALA derivatives: the rather hydrophilic ALA and MAL induce maximal PPIX formation at millimolar concentrations of the pro-drug. In contrast, a comparable amount of endogenous PPIX is synthesized by 100-μM HAL, about one order of magnitude lower than ALA/MAL. Notably, maximal levels of PPIX per GFP are achieved in a particular concentration range of ALA and MAL. Above a concentration of 1.0-mM ALA or MAL, less PPIX is generated. Therefore, the classical proposal of a "saturation" concentration of PPIX does not appear to be valid for A431 cells. As Grubinger et al.[33] showed, serum proteins present in the incubation medium can serve as extracellular acceptor (and probably storage compound) for PPIX. In case no serum proteins are available, the majority of PPIX remains within the cells as a result of its lipophilicity and might inhibit further synthesis. As an alternative hypothesis, PPIX molecules might form nonfluorescing aggregates above a threshold concentration and thereby cause the overall fluorescence to decrease. However, ALA/MAL concentrations up to 4 mM do not decrease cellular viability, even if applied for 72 h. In contrast, HAL incubation with >125 μM influences the cellular viability of A431-GFP cells [Fig. 1(b)]. As a result, the more lipophilic HAL induces comparable amounts of PPIX at lower concentrations when compared to ALA/MAL most likely due to different uptake mechanisms,[15] but the overall concentration of the PS cannot be increased above a specific value.

5 Conclusion

Automated recording of PPIX formation using a microplate reader equipped with an atmosphere regulation module represents a convenient approach for testing of new ALA derivatives or other PS pro-drugs. The excellent temporal resolution of this approach provides detailed analysis of the kinetics of PS synthesis and decomposition and overcomes the problems of a single-point determination. This study exemplifies the advantage of automated recording of PPIX formation from ALA, MAL, and HAL by showing that (i) the amount of active PS follows a three-phase kinetics, (ii) the concentration of the pro-drug determines the maximal level of intracellular PPIX and the point in time at which this maximum appears, (iii) the overall cellular PPIX concentration cannot exceed a certain value, independent of the amount of the pro-drug applied, and (iv) the more lipophilic HAL produces comparable amounts of PPIX at incubation concentrations about one order of magnitude lower compared with the hydrophilic ALA or MAL.

References

1. K. Berg et al., "Porphyrin-related photosensitizers for cancer imaging and therapeutic applications," *J. Microsc.* **218**, 133–147 (2005).
2. Q. Peng et al., "5-Aminolevulinic acid-based photodynamic therapy. Clinical research and future challenges," *Cancer* **79**, 2282–2308 (1997).
3. J. Webber, D. Kessel, and D. Fromm, "Plasma levels of protoporphyrin IX in humans after oral administration of 5-aminolevulinic acid," *J. Photochem. Photobiol. B* **37**, 151–153 (1997).
4. S. L. Marcus et al., "Photodynamic therapy (PDT) and photodiagnosis (PD) using endogenous photosensitization induced by 5-aminolevulinic acid (ALA): current clinical and development status," *J. Clin. Laser Med. Surg.* **14**(2), 59–66 (1996).
5. J. C. Kennedy, S. L. Marcus, and R. H. Pottier, "Photodynamic therapy (PDT) and photodiagnosis (PD) using endogenous photosensitization induced by 5-aminolevulinic acid (ALA): mechanisms and clinical results," *J. Clin. Laser Med. Surg.* **14**(5), 289–304 (1996).
6. C. J. Kelty et al., "The use of 5-aminolaevulinic acid as a photosensitiser in photodynamic therapy and photodiagnosis," *Photochem. Photobiol. Sci.* **1**, 158–168 (2002).
7. C. Fritsch, G. Goerz, and T. Ruzicka, "Photodynamic therapy in dermatology," *Arch. Dermatol.* **134**, 207–214 (1998).
8. H. Brunner, F. Hausmann, and R. Knuechel, "New 5-aminolevulinic acid esters–efficient protoporphyrin precursors for photodetection and photodynamic therapy," *Photochem. Photobiol.* **78**, 481–486 (2003).
9. A. Casas and A. Batlle, "Aminolevulinic acid derivatives and liposome delivery as strategies for improving 5-aminolevulinic acid-mediated photodynamic therapy," *Curr. Med. Chem.* **13**, 1157–1168 (2006).
10. J. Kloek and H. Beijersbergen van, "Prodrugs of 5-aminolevulinic acid for photodynamic therapy," *Photochem. Photobiol.* **64**, 994–1000 (1996).
11. Z. Luksiene et al., "Evaluation of protoporphyrin IX production, phototoxicity and cell death pathway induced by hexylester of 5-aminolevulinic acid in Reh and HPB-ALL cells," *Cancer Lett.* **169**, 33–39 (2001).
12. P. Uehlinger et al., "5-Aminolevulinic acid and its derivatives: physical chemical properties and protoporphyrin IX formation in cultured cells," *J. Photochem. Photobiol. B* **54**, 72–80 (2000).
13. F. J. Moloney and P. Collins, "Randomized, double-blind, prospective study to compare topical 5-aminolaevulinic acid methylester with topical 5-aminolaevulinic acid photodynamic therapy for extensive scalp actinic keratosis," *Br. J. Dermatol.* **157**, 87–91 (2007).
14. S. R. Wiegell et al., "Pain associated with photodynamic therapy using 5-aminolevulinic acid or 5-aminolevulinic acid methylester on tape-stripped normal skin," *Arch. Dermatol.* **139**, 1173–1177 (2003).
15. N. Fotinos et al., "5-Aminolevulinic acid derivatives in photomedicine: characteristics, application and perspectives," *Photochem. Photobiol.* **82**, 994–1015 (2006).
16. L. Rodriguez et al., "Mechanisms of 5-aminolevulinic acid ester uptake in mammalian cells," *Br. J. Pharmacol.* **147**, 825–833 (2006).
17. Y. Hagiya et al., "Expression levels of PEPT1 and ABCG2 play key roles in 5-aminolevulinic acid (ALA)-induced tumor-specific protoporphyrin IX (PpIX) accumulation in bladder cancer," *Photodiagn. Photodyn. Ther.* **10**, 288–295 (2013).
18. Y. Hagiya et al., "Pivotal roles of peptide transporter PEPT1 and ATP-binding cassette (ABC) transporter ABCG2 in 5-aminolevulinic acid (ALA)-based photocytotoxicity of gastric cancer cells in vitro," *Photodiagn. Photodyn. Ther.* **9**, 204–214 (2012).
19. Y. Baglo et al., "Homology modeling of human gamma-butyric acid transporters and the binding of pro-drugs 5-aminolevulinic acid and methyl aminolevulinic acid used in photodynamic therapy," *PLoS One* **8**, e65200 (2013).
20. E. Rud et al., "5-aminolevulinic acid, but not 5-aminolevulinic acid esters, is transported into adenocarcinoma cells by system BETA transporters," *Photochem. Photobiol.* **71**, 640–647 (2000).
21. F. Doring et al., "Delta-aminolevulinic acid transport by intestinal and renal peptide transporters and its physiological and clinical implications," *J. Clin. Invest.* **101**, 2761–2767 (1998).
22. H. Brunner et al., "The effects of 5-aminolevulinic acid esters on protoporphyrin IX production in human adenocarcinoma cell lines," *Photochem. Photobiol.* **74**, 721–725 (2001).
23. M. T. Wyss-Desserich et al., "Accumulation of 5-aminolevulinic acid-induced protoporphyrin IX in normal and neoplastic human endometrial epithelial cells," *Biochem. Biophys. Res. Commun.* **224**, 819–824 (1996).
24. J. Berlanda et al., "Comparative in vitro study on the characteristics of different photosensitizers employed in PDT," *J. Photochem. Photobiol. B* **100**, 173–180 (2010).
25. T. Kiesslich et al., "Uptake and phototoxicity of meso-tetrahydroxy-phenyl chlorine are highly variable in human biliary tract cancer cell lines and correlate with markers of differentiation and proliferation," *Photochem. Photobiol. Sci.* **9**, 734–743 (2010).
26. J. Wachter et al., "Influence of five potential anticancer drugs on wnt pathway and cell survival in human biliary tract cancer cells," *Int. J. Biol. Sci.* **8**, 15–29 (2012).
27. E. M. Czekanska, "Assessment of cell proliferation with resazurin-based fluorescent dye," *Methods Mol. Biol.* **740**, 27–32 (2011).
28. A. Casas and A. Batlle, "Rational design of 5-aminolevulinic acid derivatives aimed at improving photodynamic therapy," *Curr. Med. Chem. Anticancer Agents* **2**, 465–475 (2002).
29. T. Feuerstein, A. Schauder, and Z. Malik, "Silencing of ALA dehydratase affects ALA-photodynamic therapy efficacy in K562 erythroleukemic cells," *Photochem. Photobiol. Sci.* **8**, 1461–1466 (2009).
30. R. G. Tunstall et al., "Porphyrin accumulation induced by 5-aminolaevulinic acid esters in tumour cells growing in vitro and in vivo," *Br. J. Cancer* **87**, 246–250 (2002).
31. L. Wyld et al., "Factors affecting aminolaevulinic acid-induced generation of protoporphyrin IX," *Br. J. Cancer* **76**, 705–712 (1997).
32. B. Krammer and K. Uberriegler, "In-vitro investigation of ALA-induced protoporphyrin IX," *J. Photochem. Photobiol. B* **36**, 121–126 (1996).
33. M. Grubinger et al., "Accumulation of aminolevulinic acid-induced protoporphyrin IX as a photosensitizer in L-929 cells," *Res. Adv. Photochem. Photobiol.* **1**, 137–145 (2000).

Tobias Kiesslich is a university assistant at the Institute of Physiology and Pathophysiology and the Department of Internal Medicine I (Paracelsus Medical University Salzburg). He received his doctoral degree (2007) at the University of Salzburg and the *venia docendi* (physiology) in 2014 at the Paracelsus Medical University, Salzburg, Austria. Current topics of his research group include cellular mechanisms of anticancer photodynamic therapy and oncogenesis signaling pathways in gastrointestinal neoplasias.

Linda Helander, MSc, received her degree in Trondheim at NTNU (Norwegian University of Science and Technology) in 2004. She studied biophysics and has after her degree worked as a staff engineer

within molecular biology at University of Tromsø and is currently working as head of laboratory of NTNU Nanolab and finishing her PhD within the program of molecular medicine at NTNU.

Romana Illig: Biography is not available.

Christian Oberdanner received his doctoral degree in 2007 at the University of Salzburg. In his thesis he focused on apoptosis induction and reactive oxygen species. Christian joined the department for research and development at Tecan Austria in 2007 as a specialist for detection product, especially for multimode microplate readers. In 2008 he switched to the sales and marketing department, where he still works as a senior application scientist and junior product manager.

Andrej Wagner is a senior physician and gastroenterologist at the Department of Internal Medicine I (Paracelsus Medical University Salzburg). He received his doctoral degree (2003) at the University of Frankfurt a. M. Current topics of his research include clinical features and cellular mechanisms of photodynamic therapy for bile duct cancer and endoscopic submucosal resection techniques for gastrointestinal neoplasias.

Herbert Lettner is associate professor in environmental biophysics at the University of Salzburg, Austria. He is researching in radiation environmental biophysics on the transport behavior of radionuclides and radon decay products in the human body associated with radon balneotherapy. He is technical head of the Radiation Measurements Laboratory at the University of Salzburg.

Martin Jakab is received his doctoral degree at the University of Salzburg in 1996 and the *venia docendi* in physiology in 2009 at the Paracelsus Medical University (PMU), Salzburg, Austria. He is currently head of the Laboratory for Functional and Molecular Membrane Physiology (FMMP) at the PMU. His main research topics are cellular mechanisms of volume and pH regulation and their influences on stimulus-secretion-coupling, cell proliferation, migration, and phagocytosis.

Kristjan Plaetzer earned his PhD and venia docendi in biophysics at the University of Salzburg, Austria. He is interested in the cell death modes induced by PDT and cellular energetics of photo-treated cells and acquired expertise in application of photodynamic procedures based on natural substances as photosensitizers against microorganisms. He is now head of the Laboratory of Photodynamic Inactivation at the University of Salzburg (PDI-PLUS).